THORACOLUMBAR OSTEOCHONDROMA IN A PATIENT WITH MULTIPLE EXOSTOTIC CHONDRODYSPLASIA: A CASE REPORT

M.S. Asadulaev, S.V. Vissarionov, D.B. Malamashin, A.D. Nilov, T.V. Murashko
H. Turner National Medical Research Center for Children's Orthopedics and Trauma Surgery, Saint Petersburg, Russia

The results of surgical treatment of a 14-year-old female patient with a rare vertebrological disorder, multiple exostotic chondrodysplasia with spinal column involvement, are presented. Clinical, radiographic, MRI, histological and laboratory examinations were carried out. The observation revealed a massive space-occupying lesion in the spinal column with projected dimensions of 97 × 70 × 72 mm. The patient had narrowing of the intervertebral foramina with signs of compression of the L1—L2 and L2—L3 nerve roots on the left, secondary deformity and cranial displacement of the 12th rib on the left.

Key Words: multiple exostotic chondrodysplasia; vertebral osteochondroma; dyschondroplasia; children; orthopedics; spinal deformity; deformity stabilization.

Please cite this paper as: *Asadulaev MS, Vissarionov SV, Malamashin DB, Nilov AD, Murashko TV. Thoracolumbar osteochondroma in a patient with multiple exostotic chondrodysplasia: a case report. Russian Journal of Spine Surgery (Khirurgiya Pozvonochnika). 2025;22(4):74–84. In Russian. DOI: http://dx.doi.org/10.14531/ss2025.4.74-84*

Osteochondroma is one of the most common benign bone neoplasms, accounting for 20–50% of cases [1, 2]. In approximately 85% of cases, osteochondromas occur sporadically as solitary osteocartilaginous exostoses. Concurrently, in about 15% of observations, a hereditary multiple exostotic chondrodysplasia (HME) is occurs [3–5]. This condition is characterized by the development of multiple osteocartilaginous exostoses within both the peripheral and axial skeletons [6–8].

HME has an autosomal dominant inheritance pattern with incomplete penetrance in women, resulting in a slight predominance of males with this condition. The incidence of the disease is approximately 1 case per 50000 people [9, 10]. The number of exostoses, the degree and type of skeletal deformity, and the frequency of malignant transformation differ significantly even within the same family.

According to the World Health Organization Classification of Soft Tissue and Bone Tumours (5th edition), the diagnostic criteria for HME include the presence of two or more radiologically confirmed osteochondromas in the juxtaepiphyseal region of long tubular bones, combined with a positive family history and/or a germline mutation in the *EXT* gene [11].

The objective is to present a rare clinical case report of giant osteochondroma of the thoracolumbar spine in a female patient with HME.

Description of a Clinical Case Report

Female patient B. was admitted to the clinical unit at the age of 14 for a progressive, space-occupying lesion in the thoracolumbar spine. She is being treated via a federal and regional telemedicine consultation system by specialists from the Traumatology and Orthopedics Department No. 2 of the H. Turner National Medical Research Center for Children's Orthopedics and Trauma Surgery (Saint Petersburg). The patient was recommended to be hospitalized for additional examination and surgical treatment.

Case history

Since 2020, she has been receiving outpatient follow-up care at her place of residence for hereditary multiple osteocartilaginous exostoses. In 2025, at the age of 13, she underwent surgery for exostosis of the right lower leg.

Life history

The diagnosis was made at the age of nine. No significant allergic history. She was born during the mother's third pregnancy, which was complicated by threatened miscarriage and diseases (anemia, gestosis). It was the mother's first delivery, which was at term. The girl's birth weight was 3370 g, and her length was 52 cm. No family history of exostotic chondrodysplasia was reported.

During the examination, a pronounced space-occupying lesion in the thoracolumbar spine is determined, significantly protruding in the projection of the left paravertebral and lumbar region (Fig. 1).

Diagnostic findings

When the patient was admitted, she underwent a comprehensive laboratory examination, including a complete blood count, blood clotting test, blood type and Rh factor testing, biochemical blood count, and assessment of bleeding time. To identify the presence of space-occupying lesions in the extremities and axial skeleton, a digital panoramic radiography was performed in two planes (Fig. 2).

The patient showed deformity of the L1–L4 lumbar vertebrae with disruption of the trabecular pattern and subchondral regions with massive cortical thickening at the level of the arches and lateral aspects on the left, appearing as a bone-density mass with uneven min-

eralization, with projection dimensions of 97 × 70 × 72 mm, with irregular well-defined margins. There were secondary deformity and cranial displacement of the left 12th rib. There was a secondary right-sided scoliotic deformity of the lumbar spine up to 10° according to the Cobb. A symmetrical lumbosacral transitional vertebra was noted.

Neurological examination findings: consciousness is clear; oriented to time and place. Muscle tone was physiological and symmetrical. Muscle strength was reduced in the lower extremities, in the proximal segments (during exercise tests). Sensory impairment was noted along the lateral surface of the right lower leg (status post-surgery for exostosis of the right lower extremity in February 2025). Hypotrophy of the left calf muscles, the left foot was smaller than the right one. Tendon reflexes were brisk, knee reflexes were reduced, mainly on the left. No pathological reflexes. Normal bowel and bladder functions. The patients walked independently; ability to walk on toes and heels was maintained.

A preoperative multi-slice computed tomography (MSCT) was performed on the patient for localization diagnosis of the neoplasm and to plan rational approach to the neoplasm (Fig. 3).

In the preoperative period, the patient underwent MRI to identify the soft tissue component of the space-occupying lesion and to determine possible involvement of neural structures (Figs. 4–6).

The size of the cartilage component at the top of the osteochondroma varies up to 0.8 cm. In children, the thickness of the cartilaginous membrane can reach 3 cm [21]. The presence of lobularity in the structure of the pathological formation without cystic components (the main mass of the formation has MR signal characteristics corresponding to bone marrow and adipose tissue), with no edema of the adjacent soft tissues. Minor secondary deformity of the posterior wall of the spinal canal at the L1–L2 level, without intracanal changes. Paravertebral soft tissues were secondarily displaced by the formation, including the *m. psoas major sinistra*.

After a comprehensive examination, the findings were discussed by specialists from the Traumatology and Orthopedics Department No. 2 of the H. Turner National Medical Research Center for Children's Orthopedics and Trauma Surgery. Considering the size of the space-occupying lesion and its potential malignancy, a decision was made to perform

Fig. 1
The appearance of a patient, 14 years old, female. Clinical examination revealed a space-occupying lesion in the thoracolumbar spine, there is the line of the spinous processes closer to the posterior midline of the body. Palpation of subcutaneous tissues revealed a bone-dense, non-displaceable lesion; skin is movable: **a** – back view; **b** – side view (left); **c** – side view (right)

Fig. 2
Panoramic radiography of the skeleton of a 14-year-old female patient in the anteroposterior **(a)** and lateral **(b)** planes: typical signs of osteocartilaginous exostoses (highlighted in red) of the long tubular bones (humeral, femoral) and flat bones (solitary in the ribs, pelvic bones – left pubic bone, lumbar vertebrae)

total removal of the lesion, correction, and stabilization of the spinal motion segment using a posterior multi-level instrumentation.

Surgery

The surgery was performed under general combined anesthesia. Patient positioning: prone with decompression of the anterior chest and abdominal wall (Fig. 7a). A skin incision was made over the center of the space-occupying lesion (left paravertebral) at the level of the T12

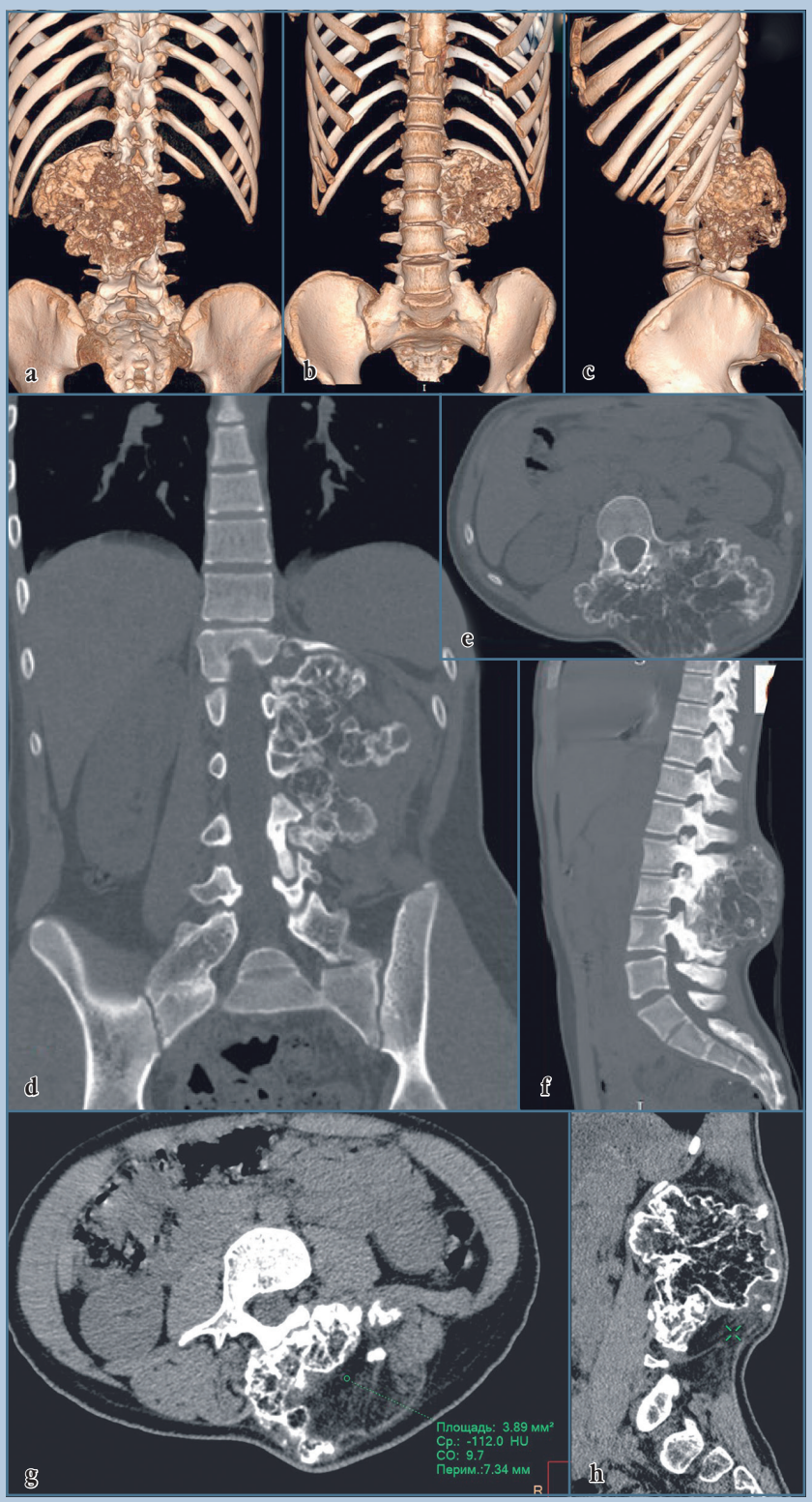

Fig. 3
CT scan of a patient, 14 years old, female: 3D image of the lower thoracic and lumbar spine **(a–c)** and multiplanar reconstructions in the frontal, sagittal and axial planes **(d–h)**. The following parameters are reliably assessed: localization (originating from the posterior structures of L2, S > D – spinous process, transverse process and superior and inferior articular processes), dimensions of the bone lesion of the lumbar vertebrae (112 × 135 × 70 mm – height × width × anteroposterior size), changes in the cortical layer (integrity is not violated, sclerotic, 'cauliflower' type deformation), the condition of the spinal canal (without intracanal spread of the pathological bone tissue), adjacent sections of the vertebrae and ribs (secondary ankylosis of the L1–L2 intervertebral joints, arthrosis of the L1–L3 intervertebral joints; dislocation with its displacement forward and atrophy associated with pressure of the 12th rib on the left), soft tissues (fatty degeneration of muscle tissue adjacent to the lesion)

to L4 vertebrae, with a length of 16 cm. The soft tissues were dissected layer by layer; skeletization of the space-occupying lesion was performed using both blunt and sharp dissection (Fig. 7b).

Considering the massive size of the osteocartilaginous lesion, the pathological tissue was removed by piecemeal resection using Luer and Kerrison bone rongeurs. Hemostasis was achieved with bone wax and a bipolar coagulator. The length of the posterior spinal canal wall defect was 72 mm. Three facet joints on the left side were resected. The extent of instrumentation was determined by the volume of pathological tissue resection. After resection of the pathological tissue, transpedicular bone channels were formed using the freehand technique in the bodies of the L1, L2, and L3 vertebrae on the right side from the line of the spinous processes, and in the bodies of the T12 and L3 vertebrae on the left side. This formation of bone channels for transpedicular support elements of the instrumentation is associated with the volume of pathologically altered bone structures of the spinal column being removed in this area. Manual and radiological control was performed. The position of the radiological markers was correct and accurate; the walls of the bone channels were formed. Five transpedicular support elements were placed into the formed bone channels. The diameter of the rod was 5.5 mm. The different levels of instrumentation were determined by the extent of the pathological process and the need to remove the damaged bone structures within the healthy tissues. Intraoperative radiological control showed that the system was stable and the implant position was correct (Fig. 8).

Wound hemostasis. Ensuring the absence of foreign bodies in the surgical field. A wound drainage system was placed. The surgical wound was closed in layers using interrupted sutures. A continuous suture for the subcutaneous tissue and skin.

The surgery lasted 245 minutes, with intraoperative blood loss volume of 1800.0 ml. The child's neurological status after postanesthetic recovery was at the preoperative level.

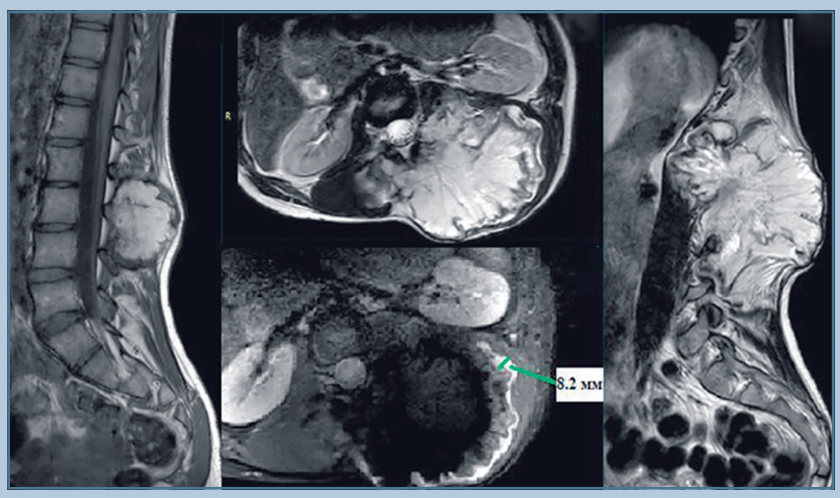

Fig. 4
MRI image of the lumbosacral spine of a 14-year-old female patient: sagittal and axial images in STIRTSE mode and T2-WI (view of a large exophytic osteocartilaginous lesion – osteochondromas of the posterior structures of the lumbar spine, S > D, osteochondromas at the L1–L2 level in the axial plane)

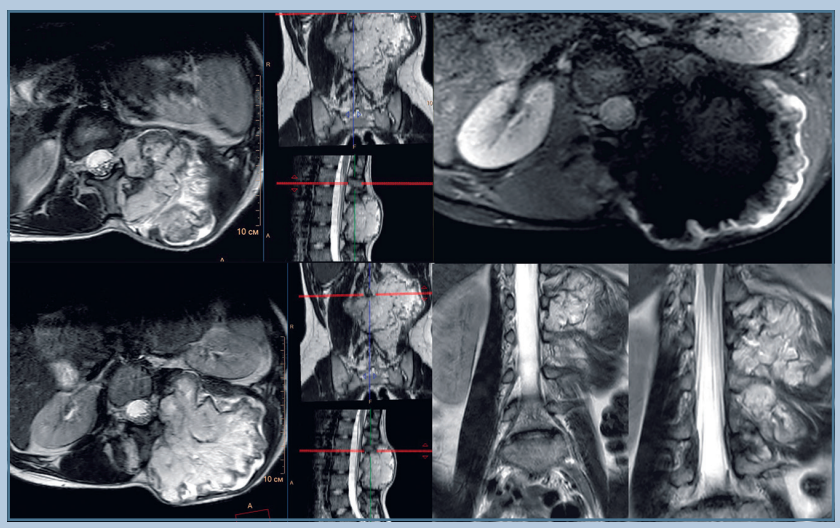

Fig. 5
MRI image of the lumbar spine: axial images at the L1–L2 level (T2-WI, STIR mode) and L2–L3 level (T2-WI); on coronal T2-WI sections, a bone lesion originating from the left L2 vertebral pedicle with deformation – remodeling and narrowing of the intervertebral foramen on the left (with signs of compression of the L1–L2 and L2–L3 nerve roots on the left)

The postoperative course was smooth. Considering the extensive cavity of the wound after removal of the space-occupying lesion, the duration of drainage was extended to 96 hours. The total amount of discharge since the surgery was up to 800.0 ml of serosanguineous origin. Preventive antibiotics treat-

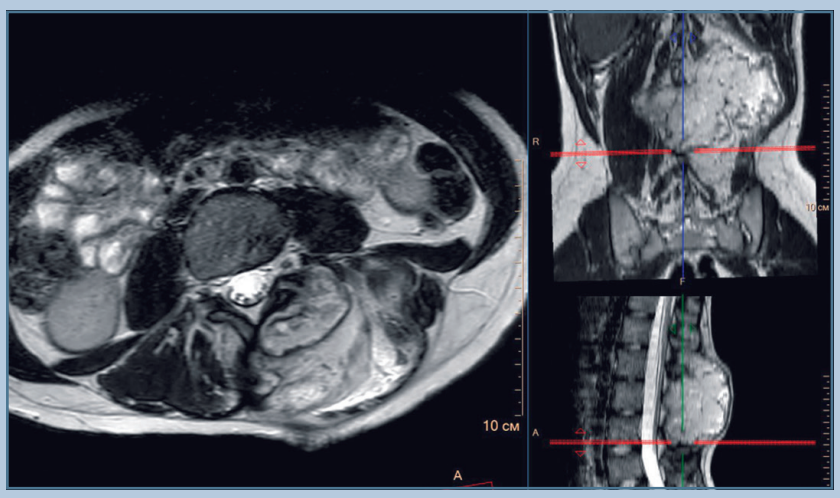

Fig. 6
Axial T2-WI of the L4–L5 level, performing deformation of the intervertebral foramen with an atypical position of the root on the left: displaced anteriorly and medially by the bone lesion of the posterior structures of the lumbar vertebrae

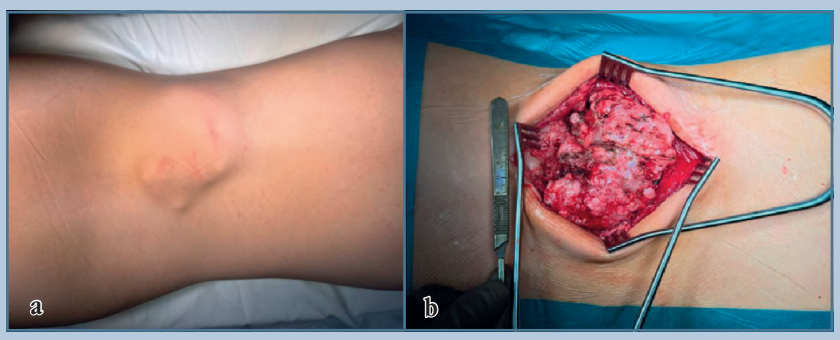

Fig. 7
The view of the surgical site after the patient positioning **(a)** and the view of the pathological lesion after approach performing **(b)**

ment was administered for 48 hours. The patient was mobilized on day 2 after the surgery. Post-hemorrhagic anemia was noted in the early postoperative period. The patient received conservative treatment (physical therapy, breathing exercises) and symptom management.

After the child was adapted to vertical load, radiological and MSCT control were performed on day 5 after surgery (Figs. 9–11).

The postoperative wound healed by primary intention, and no suture removal was required. The patient has adapted to vertical load (Fig. 12).

The excised tissue was sent to the pathology laboratory for the diagnosis verification. The results of the histological examination are given in Fig. 13.

Prognosis

Considering the patient's age and ongoing bone growth, follow-up monitoring is planned.

Discussion

Most patients are diagnosed with HME at the age of 5–12 years [6, 12]. In some patients, the disease may be asymptomatic, with several small masses, or manifest as significant bone deformity associated with multiple large osteochondromas [12]. Hereditary multiple exostoses can affect any bone in the body. The most commonly affected areas are the distal femur, proximal and distal tibia, wrist and hands, humerus, pelvis, and ribs [6, 12].

Hereditary multiple exostoses are considered to be the result mutations in the *EXT1*, *EXT2*, or *EXT3* genes on chromosomes 8q24 (*EXT1*), 11p11-13 (*EXT2*), and 19p *(EXT3*) 4,5 [6, 13]. Histologically, it is an osteophyte connected with bone marrow and the cortical layer of bone structures, and having a cartilaginous covering in the peripheral regions [14]

Aside from their multiplicity, the visualized features are identical to those of solitary osteochondromas [6, 14]. The distribution of affected areas along the body can vary a lot: some authors say the typical pattern is bilateral and symmetrical, while others report a clear predominance of unilateral pattern [15].

Localization of osteochondroma in the vertebral column is a relatively rare pathology, accounting for approximately 1% of cases [16]. In the structure of HME, exostoses in the spine are found in 7–9% of clinical cases. At the same time, osteochondroma can be found anywhere along the spine. However, it is most common in the cervical spine, especially at the C2 level.

Solitary exostosis is usually diagnosed between the ages of 20 and 30, while HME is diagnosed at an earlier age [18]. Early diagnosis of the disease in the spine occurs when the osteochondroma grows toward the spinal canal or intervertebral foramen, resulting in the development of neurological disorders [18].

Unlike osteochondromas of the upper and lower extremities, small spinal osteochondromas are challenging to diagnose using radiography and require additional imaging tests, such as MSCT and MRI [6, 7].

Complications associated with HME are similar to those associated with solitary osteochondromas and include risks of compression of blood vessels and neural structures, fractures of the exostosis, reactive changes in the muscular-liga-

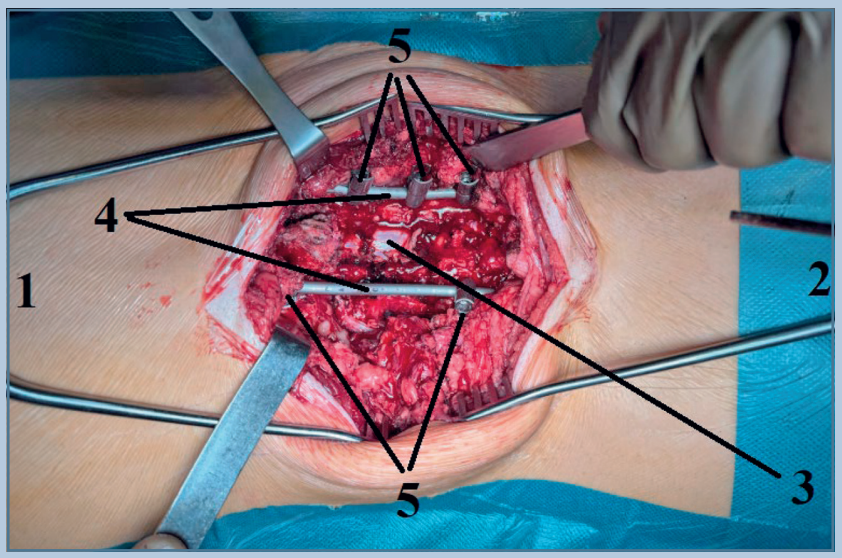

Fig. 8
The view of the surgical site after total removal of the space-occupying lesion and stabilization of the vertebrae in the resection area with a multi-level spinal instrumentation: *1* – head end of the wound; *2* – foot end of the wound; *3* – dural sac (laminectomy area); *4* – rods of the multi-level instrumentation (diameter of 5.5 mm); *5* – supporting elements of the instrumentation

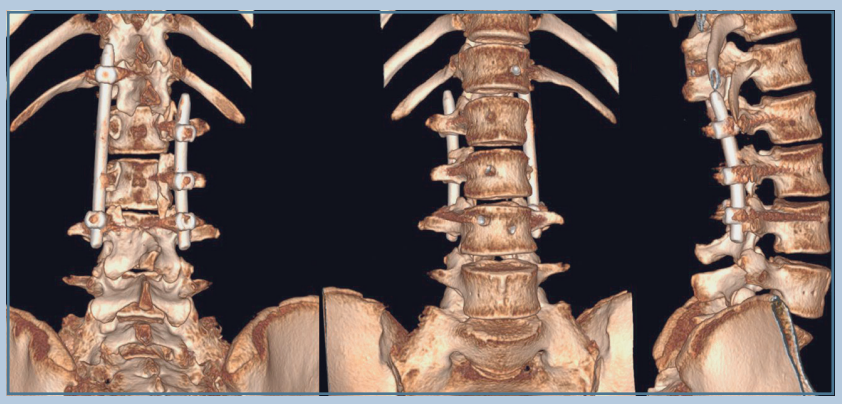

Fig. 10
A series of axial sections during the construction of multiplanar and volumetric reconstructions of the lumbar spine are used to determine the condition after surgical treatment; resection of the osteocartilaginous exostosis of the L2 vertebral spinous process was performed within the unchanged bone tissue; fixation with a 2-rod multi-level instrumentation; the spinal canal is passable throughout its entire length; no areas of bone density were detected intracanally

Fig. 9
Panoramic radiography of a 14-year-old female patient in the anteroposterior **(a)** and lateral **(b)** planes (under static load): the spinal axis in the frontal plane is not curved, without pronounced pathological rotation of the vertebrae; the intervertebral ratio is preserved, unclear imaging of the roots of the lumbar vertebral arches on the left; the height of the vertebral bodies and intervertebral foramen is preserved; the endplates of the thoracic and lumbar vertebral bodies are clear and smooth; the instrumentation is installed – pedicle screws at the T12S, L1D, L2D, L3DS; the sagittal plane image shows that the curvatures are smoothed, the posterior vertebral line is even.

mentous apparatus, secondary skeletal deformities, secondary osteoarthritis, and progression to malignancy [4–6].

Progression to malignancy occurs more frequently in patients with HME (20% of cases) than in cases of solitary osteochondromas (1% of cases) [19]. The frequency of progression ranges from 3–5% to 25% [20]. Radiological and clinical signs indicating malignant (sarcomatous) transformation of osteochondroma include growth after skeletal maturation, increased accumulation of radiopharmaceutical agent during scintigraphy, cortical destruction, the onset of severe pain in the area of exostosis after skeletal maturation, and an increased volume of the soft tissue component – thickening

Fig. 11
MSCT image of a 14-year-old female patient in multiplanar reconstruction mode: **a** – position of the supporting elements in the roots of the vertebral arches; **b** – position of the supporting element of the instrumentation at the level of the L1 vertebra; **c** – bone defect of the posterior bone structures in the area of removal of the space-occupying lesion

of the cartilage covering by more than 1.5 cm [20, 21].

The reported clinical case of giant osteochondroma of the spine in a patient with HME illustrates the rare localization of the tumor in the posterior bone structures of the thoracolumbar spine and highlights the range of complications associated with axial skeletal lesion in children [22].

Spinal localization of HME is less frequent than in cases involving long bones. According to the literature [23, 24], approximately 7–9% of osteochondromas in HME are located in the vertebrae. Approximately half of these osteochondromas are located in the cervical spine, predominantly in the dorsal bone structures. These data emphasize the unusual nature and significance of our clinical case.

Diagnostic challenges in this area are associated with the anatomical complexity of spinal imaging: radiography does not allow for a complete evaluation of the extent and severity of the pathological process, as well as the interaction between the affected area and nearby structures. Meanwhile, spine CT provides an accurate topical assessment, while MRI characterizes the cartilage component of the lesion and signs of myelopathy [21]. The combined use of CT and MRI techniques is essential for planning treatment for patients with spinal osteochondromas [25]. In our case, it was MSCT and MRI that made it possible to verify the fixation of the lesion on the posterior structures of the L2 vertebra and evaluate the absence of intracanal growth.

Patients with this pathology require oncological alertness. According to the literature [21, 25, 26], a cartilage cap thickness of more than 1.5–2.0 cm in adults or growth of the lesion after skeletal maturation may be associated with a risk of secondary chondrosarcoma. Simultaneously, it should be noted that in children, a thickness of up to 3 cm may remain within the normal range, which requires interpretation based on the patient's age [27]. In our study, there were no MRI signs of malignant transformation, which was confirmed by histopathological examination. The total risk of malignancy in HME ranges from 2% to 4% in the patient population (significantly higher than in solitary osteochondroma), with a prevalence of transformation in the pelvic region and proximal region of femur [21]. However, malignancy in the spine is rarely described [7, 28].

The treatment strategy in this situation is the following: total removal of the lesion with mandatory resection of the lesion bed to prevent recurrence and obtain a definitive morphological conclusion. The strategy coincides with the data from clinical series and reviews, which recommend complete wide excision for symptomatic spinal osteochondromas and in cases of extensive defects or the threat of instability, simultaneous instrumented stabilization is indicated [24]. In our case, the necessity for multi-level fixation was justified by the extensive resection performed and the risk of segmental instability of the spinal motion segments in this area.

The long-term prognosis for adolescents remains unpredictable: despite the radical intervention and satisfactory immediate outcomes, the risk of recurrence after complete removal of the cartilage cap is low, but long-term outcomes of deformity or instability and growth patterns require follow-up. After proper resection, recurrences are rare, and neurological symptoms, if any, regress in most patients. Considering the systemic nature of HME and possible multifocality in the axial skeleton, a multidisciplinary management model (orthopedic spine surgeon, neurosurgeon, radiologist,

pathologist, oncologist, geneticist) with a low threshold for extended imaging when pain syndrome, neurological symptoms, or growth of the lesion appear.

Conclusion

A case of giant osteochondroma of the posterior bone structures of the thoracolumbar spine in a patient with HME demonstrates an atypical localization of the tumor. CT and MRI are necessary in this situation to confirm the localization and evaluate the extent of cartilage covering. Total

Fig. 12
Appearance of a 14-year-old female patient after surgical treatment, the line of postoperative paravertebral incision is without signs of inflammation, healing by primary tension: **a** – back view; **b** – side view; **c** – half-turned view

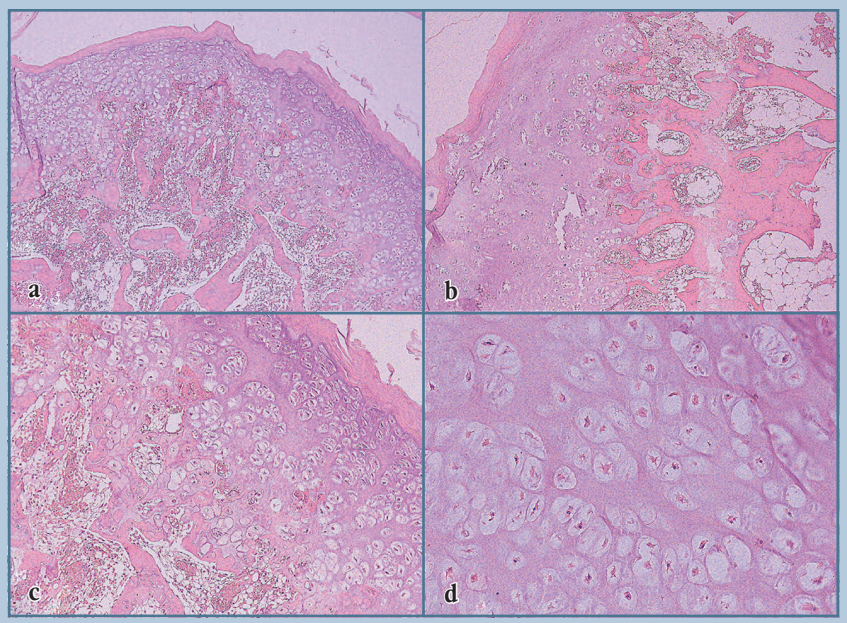

Fig. 13
Histological examination results: bone tissue fragments are determined, represented by bone trabeculae with perifocal osteoclastic response and a small number of giant multinucleated cells of the osteoclastic type; on the surface of the bone trabeculae, a cartilage cap is noted, formed by mature hyaline cartilage with multiple chondrocytes evenly distributed in the ground substance; chondrocytes are located mainly randomly in the form of isolated cells and groups of different sizes; hematopoietic bone marrow cells with an admixture of adipocytes are found in wide intertrabecular spaces; areas of secondary ossification in the subchondral zones: **a, b** – overview micrographs of osteocartilaginous exostosis, hematoxylin and eosin, magnification 50; **c** – osteocartilaginous zone formed by bone trabeculae with areas of hyaline cartilage cap, hematoxylin and eosin, magnification 100; **d** – area of hyaline cartilage with numerous chondrocytes located in a basophilic matrix, hematoxylin and eosin, magnification 200

resection with simultaneous stabilization provided satisfactory immediate treatment outcomes and correction of secondary changes. The risk of malignant transformation in HME is low, but it requires oncological alertness and morphological verification of the resected specimen. Adolescence and ongoing bone growth require ongoing follow-up of the pathological condition by an oncologist, orthopedic spine surgeon, pediatrician, and neurologist to ensure timely determination of optimal surgical treatment with consideration of the extent of the pathology, clinical manifestations, and skeletal growth prospects.

Limitations of the study: the article considers the immediate surgical outcomes for the patient; there is no data on long-term follow-up.

The authors express their gratitude to the medical and nursing staff of the H. Turner National Medical Research Center for Children's Orthopedics and Trauma Surgery.

Funding: The study was supported by the Ministry of Health of the Russian Federation under the state assignment (R&D project: "Comprehensive Treatment of Children with Congenital Chest and Spinal Deformities and Instability of the Sternocostal Complex"; registration No. 1023021600029-8-3.2.10). The study was approved by the local ethics committee (Protocol No. 20-3 dated November 20, 2020). Written informed consent was obtained from the patient / medical proxy. The authors declare that they have no conflict of interest. All authors contributed significantly to the research and preparation of the article, read and approved the final version before publication.

References

1. **Alabdullrahman LW, Mabrouk A, Byerly DW.** Osteochondroma. In: *StatPearls [Internet]*. Treasure Island (FL): StatPearls Publishing, 2025. PMID: 31335016.
2. **Vasilev IA, Maysigov MN, Logvinov AN, Frolov AV, Bessonov DA, Ilyin DO, Korolev AV.** Treatment of a patient with massive osteochondral exostosis of the radial neck: clinical case. *Journal of Clinical Practice*. 2024;15(2):81–88. DOI: 10.17816/clinpract626315 EDN: WVHPZK
3. **Tepelenis K, Delinasios GJ, Zoga A, et al.** Osteochondromas: an updated review of epidemiology, pathogenesis, clinical presentation, radiological features and treatment options. *In Vivo*. 2021;35:681–691. DOI: 10.21873/invivo.12308
4. **Malamashin DB, Mushkin AYu, Glukhov DA, Snishchuk VP.** Enchondromatosis with cervical spine involvement in children: small series and review. *Russian Journal of Spine Surgery (Khirurgiya Pozvonochnika)*. 2022;19(1):56–62. DOI: 10.14531/ss2022.1.56-62 EDN: LMCZXB
5. **Malamashin DB, Mushkin AYu.** Multiple chondromatosis of bones (Ollier disease) with damage to the costal frame in cjildren (analysis of a small clinical series). *Medical Alliance*. 2021;9(4):87–98. DOI: 10.36422/23076348-2021-9-4-87-98 EDN: DDVKHJ
6. **Chigvaria NG, Pozdeev AP, Bergaliev AN.** Metaphyseal fibrous defects and nonossifying bone fibroma in children: clinical types and treatment. *Pediatric Traumatology, Orthopaedics and Reconstructive Surgery*. 2014;2(2):12–25. DOI: 10.17816/PTORS2212-25 EDN: SJFIOP
7. **D'Arienzo A, Andreani L, Sacchetti F, Colangeli S, Capanna R**. Hereditary multiple exostoses: current insights. *Orthop Res Rev*. 2019;11:199–211. DOI: 10.2147/ORR.S183979
8. **Bukowska-Olech E, Trzebiatowska W, Czech W, Drzymała O, Fr k P, Klarowski F, Kłusek P, Szwajkowska A, Jamsheer A**. Hereditary multiple exostoses – a review of the molecular background, diagnostics, and potential therapeutic strategies. *Front Genet*. 2021;12:759129. DOI: 10.3389/fgene.2021.759129
9. **Ryzhikov DV, Vissarionov SV, Pershina PA.** Surgical correction of contractureand subluxation of the hipjoint in children with hereditary multiple exostosis. *Modern Problems of Science and Educatio*n. 2024;(3):22. DOI: 10.17513/spno.33438 EDN: JVBSPQ
10. **Rueda-de-Eusebio A, Gomez-Pena S, Moreno-Casado MJ, Marquina G, Arrazola J,** Crespo-Rodriguez AM. Hereditary multiple exostoses: an educational review. *Insights Imaging*. 2025;16:46. DOI: 10.1186/s13244-025-01899-6
11. Soft Tissue and Bone Tumours. WHO Classification of Tumours, 5th Edition, Vol. 3. WHO, 2020. ISBN: 9789283245025
12. **D'Ambrosi R, Ragone V, Caldarini C, Serra N, Usuelli FG, Facchinin RM.** The impact of hereditary multiple exostoses on quality of life, satisfaction, global health status, and pain. *Arch Orthop Trauma Surg*. 2017;137:209–215. DOI: 10.1007/s00402-016-2608-4
13. **Philippe C, Porter DE, Emerton ME, Wells DE, Simpson AH, Monaco AP.** Mutation screening of the EXT1 and EXT2 genes in patients with hereditary multiple exostoses. *Am J Hum Genet*. 1997;61:520–528. DOI: 10.1086/515505
14. **Garcia RA, Inwards CY, Unni KK.** Benign bone tumors - recent developments. *Semin Diagn Pathol*. 2011;28:73–85. DOI: 10.1053/j.semdp.2011.02.013
15. **Gaillard F, Hacking C, Glick Y, et al.** Hereditary multiple exostoses. Reference article, Radiopaedia.org. URL: https://doi.org/10.53347/rID-1445. Accessed on 14 Sep 2025.
16. **Sciubba DM, Macki M, Bydon M, Germscheid NM, Wolinsky JP, Boriani S, Bettegowda C, Chou D, Luzzati A, Reynolds JJ, Szövérfi Z, Zadnik P, Rhines LD, Gokaslan ZL, Fisher CG, Varga PP.** Long-term outcomes in primary spinal osteochondroma: a multicenter study of 27 patients. *J Neurosurg Spine*. 2015;22:582–588. DOI: 10.3171/2014.10.SPINE14501
17. **Rajakulasingam R, Murphy J, Botchu R, James SL.** Osteochondromas of the cervical spine – case series and review. *J Clin Orthop Trauma*. 2020;11:905–909. DOI: 10.1016/j.jcot.2019.12.014
18. **Aithala JP.** C2 intraspinal osteochondroma causing spinal cord compression in a patient with multiple hereditary exostoses. *Indian Spine J*. 2022;5:137–141. DOI: 10.4103/ISJ.ISJ_55_20
19. **Bogar WC.** Osteochondroma of the knee. *J Manipulative Physiol Ther*. 1993;16:253–255.
20. **Sonne-Holm E, Wong C,** Sonne-Holm S. Multiple cartilaginous exostoses and development of chondrosarcomas – a systematic review. *Dan Med J*. 2014;61:A4895.
21. **Murphey MD, Choi JJ, Kransdorf MJ, Flemming DJ, Gannon FH.** Imaging of osteochondroma: variants and complications with radiologic-pathologic correlation. *Radiographics*. 2000;20:1407–1434. DOI: 10.1148/radiographics.20.5.g00se171407
22. **Pawar ED, Gavhale S, Bansal S, Dave H, Yadav AK, Akshay KS.** Solitary osteochondroma of posterior elements of the spine: a rare case report. *J Orthop Case Rep*. 2020;10:1–5. DOI: 10.13107/jocr.2020.v10.i08.1832
23. **Rajakulasingam R, Murphy J, Botchu R, James SL.** Osteochondromas of the cervical spine - case series and review. *J Clin Orthop Trauma*. 2020;11:905–909. DOI: 10.1016/j.jcot.2019.12.014

24. **Yakkanti R, Onyekwelu I, Carreon LY, Dimar JR 2nd.** Solitary osteochondroma of the spine - a case series: review of solitary osteochondroma with myelopathic symptoms. *Global Spine J.* 2018;8:323–339. DOI: 10.1177/2192568217701096
25. **Riahi H, Mechri M, Barsaoui M, Bouaziz M, Vanhoenacker F, Ladeb M.** Imaging of benign tumors of the osseous spine. *J Belg Soc Radiol.* 2018;102:13. DOI: 10.5334/jbsr.1380
26. **Bernard SA, Murphey MD, Flemming DJ, Kransdorf MJ.** Improved differentiation of benign osteochondromas from secondary chondrosarcomas with standardized measurement of cartilage cap at CT and MR imaging. *Radiology.* 2010;255:857–865. DOI: 10.1148/radiol.10082120
27. **Kim HK, Horn P, Dardzinski B, Kim DH, Laor T.** T2 relaxation time mapping of the cartilage cap of osteochondromas. *Korean J Radiol.* 2016;17:159–165. DOI: 10.3348/kjr.2016.17.1.159
28. **Fei L, Ngoh C, Porter DE.** Chondrosarcoma transformation in hereditary multiple exostoses: A systematic review and clinical and cost-effectiveness of a proposed screening model. *J Bone Oncol.* 2018;13:114–122. DOI: 10.1016/j.jbo.2018.09.011

Address correspondence to:
Asadulaev Marat Sergeyevich
H. Turner National Medical Research Center
for Children's Orthopedics and Trauma Surgery,
64-68 Parkovaya str., Pushkin, Saint Petersburg, 196603, Russia,
marat.asadulaev@yandex.ru

Received 14.09.2025
Review completed 09.10.2025
Passed for printing 06.11.2025

Marat Sergeyevich Asadulaev, MD, PhD, traumatologist-orthopaedist, researcher in the Department of Spine, Spinal Cord and Chest Pathology, H. Turner National Medical Research Center for Children's Orthopedics and Trauma Surgery, 64-68 Parkovaya str., Pushkin, Saint Petersburg, 196603, Russia, eLibrary SPIN: 3336-8996, ORCID: 0000-0002-1768-2402, marat.asadulaev@yandex.ru;
Sergei Valentinovich Vissarionov, DMSc, Prof., Director, Professor of the Department of Pediatric Traumatology and Orthopedics, H. Turner National Medical Research Center for Children's Orthopedics and Trauma Surgery, 64-68 Parkovaya str., Pushkin, Saint Petersburg, 196603, Russia, eLibrary SPIN: 7125-4930, ORCID: 0000-0003-4235-5048, vissarionovs@gmail.com;
Denis Borisovich Malamashin, MD, PhD, traumatologist-orthopaedist, Clinic of Spinal Pathology and Neurosurgery, H. Turner National Medical Research Center for Children's Orthopedics and Trauma Surgery, 64-68 Parkovaya str., Pushkin, Saint Petersburg, 196603, Russia, eLibrary SPIN: 9650-6020, ORCID: 0000-0002-7356-6860, malamashin@mail.ru;
Alexander Dmitryevich Nilov, MD, pathologist, H. Turner National Medical Research Center for Children's Orthopedics and Trauma Surgery, 64-68 Parkovaya str., Pushkin, Saint Petersburg, 196603, Russia, eLibrary SPIN: 8289-3490, ORCID: 0009-0005-8845-7009, sb097@mail.ru;
Tatiana Valeyevna Murashko, MD, radiologist, H. Turner National Medical Research Center for Children's Orthopedics and Trauma Surgery, 64-68 Parkovaya str., Pushkin, Saint Petersburg, 196603, Russia, eLibrary SPIN: 9295-6453, ORCID: 0000-0002-0596-3741, popova332@mail.ru.